

Spin fluctuations from Bogoliubov Fermi surfaces in the superconducting state of S-substituted FeSe

Zhongyu Yu^{1,9}, Koya Nakamura^{1,9}, Kazuya Inomata¹, Xiaoling Shen^{2,3}, Taketora Mikuri³, Kohei Matsuura^{4,6}, Yuta Mizukami^{4,7}, Shigeru Kasahara^{5,8}, Yuji Matsuda⁵, Takasada Shibauchi⁴, Yoshiya Uwatoko³ & Naoki Fujiwara¹✉

The study of the iron-based superconductor, FeSe, has resulted in various topics, such as the interplay among superconductivity, nematicity, and magnetism, Bardeen-Cooper-Schrieffer Bose-Einstein-condensation (BCS-BEC) crossover, and Fulde-Ferrell-Larkin-Ovchinnikov (FFLO) superconductivity. Recently, topologically protected nodal Fermi surfaces, referred to as Bogoliubov Fermi surfaces (BFSs), have garnered much attention. A theoretical model for the S-substituted FeSe system demonstrated that BFSs can manifest under the conditions of spin-orbit coupling, multi-band systems, and superconductivity with time-reversal symmetry breaking. Here we report the observation of spin fluctuations originating from BFSs in the superconducting (SC) state via ⁷⁷Se-nuclear magnetic resonance measurements to 100 mK. In a heavily S-substituted FeSe, we found an anomalous enhancement of low-energy spin fluctuations deep in the SC state, which cannot be explained by an impurity effect. Such unusual behavior implies the presence of significant spin fluctuations of Bogoliubov quasi-particles, which are associated with possible nesting properties between BFSs.

¹Graduate School of Human and Environmental Studies, Kyoto University, Yoshida-Nihonmatsu-cho, Sakyo-ku, Kyoto 606-8501, Japan. ²Department of Physics, Yokohama National University, 79-1 Tokiwadai, Hodogaya-ku, Yokohama 240-8501 Kanagawa, Japan. ³Institute for Solid State Physics, University of Tokyo, 5-1-5 Kashiwanoha, Kashiwa 277-8581 Chiba, Japan. ⁴Department of Advanced Materials Science, University of Tokyo, 5-1-5 Kashiwanoha, Kashiwa 277-8561 Chiba, Japan. ⁵Department of Physics, Kyoto University, Kitashirakawa Oiwake-cho, Sakyo-ku, Kyoto 606-8502, Japan. ⁶Present address: Department of Applied Physics, University of Tokyo, 7-3-1 Hongo, Bunkyo-ku, Tokyo 113-8656, Japan. ⁷Present address: Graduate School of Science, Department of Physics, Tohoku University, Sendai 980-8578 Miyagi, Japan. ⁸Present address: Research Institute for Interdisciplinary Science, Okayama University, Okayama 700-8530, Japan. ⁹These authors contributed equally: Zhongyu Yu, Koya Nakamura. ✉email: fujiwara.naoki.7e@kyoto-u.ac.jp

The study of the iron-based superconductor, FeSe, has resulted in various topics, such as the appearance of superconductivity in the electronic nematic phase without magnetism, Bardeen-Cooper-Schrieffer Bose-Einstein-condensation (BCS-BEC) crossover, and Fulde-Ferrell-Larkin-Ovchinnikov (FFLO) superconductivity at very high magnetic fields¹. FeSe has unique features among iron-based superconducting (SC) systems, such as the formation of Fermi surfaces with unconnected small hole and electron pockets with very small Fermi energies, and the absence of magnetism in the nematic phase where four-fold symmetry is broken on the FeSe plane. These features are maintained by isovalent substitution in FeSe_{1-x}S_x up to the nematic quantum critical point (QCP) ($x_c \approx 0.17$). In contrast to magnetism, the SC state spreads across a wide S-substitution regime² and that developed in the nematic phase has a higher T_c (~ 9 K) than that in the tetragonal phase ($x > x_c$) with four-fold symmetry ($T_c \sim 4$ K). According to recent angle-resolved-photo-emission-spectroscopy (ARPES) measurements for pure FeSe, the hole pocket near the zone center (Γ point) exhibits an ellipsoidal shape, and its SC gap has a two-fold symmetric character with possible nodal points³. This implies that *s*- and *d*-wave components are significantly mixed in the nematic phase. With increasing S-concentration levels, the nematic fluctuations are strongly enhanced, and the transport properties exhibit non-Fermi liquid behavior. Accompanied by such changes near the nematic QCP, a change in the SC-gap structure has been suggested based on the field dependence of the specific heat and thermal conductivity⁴. Moreover, a marked change in the SC gap has been observed in systematic scanning-tunneling-spectroscopy (STS) studies^{5,6}. The SC-gap spectrum showed a small zero-energy conductance below x_c , whereas it was significantly enhanced above x_c .

Recently, Setty, et al. proposed a theoretical model for a system with spin-orbit coupling, multi-band structures, and time-reversal symmetry breaking (TRSB), and suggested that topologically protected nodal Fermi surfaces, referred to as Bogoliubov Fermi surfaces (BFSs), are induced in the SC state^{7,8}. The appearance of the nonzero DOS in the specific heat and thermal conductance measurements in a heavily S-substituted regime can be explained by the formation of BFSs. TRSB required for BFSs was recently suggested from muon spin relaxation measurements⁹. The existence of BFSs is a significantly important topic because it is deeply

associated with SC pairing symmetry. Furthermore, whether interband interactions exist between BFSs remains an open question. We investigated the formation of BFSs in the SC state and interband interactions from the perspective of low-energy magnetic fluctuations using ⁷⁷Se-nuclear magnetic resonance (NMR) down to 100 mK. Deep in the SC state, we found the presence of spin fluctuations of Bogoliubov quasiparticles, which are associated with possible nesting properties between BFSs.

Results and discussion

Previous NMR measurements were performed mainly above T_c for pure bulk FeSe¹⁰⁻¹⁸ and S-substituted FeSe¹⁹⁻²⁴. Studies have primarily focused on the relationship between superconductivity, nematicity, and magnetic order above T_c . We performed ⁷⁷Se-NMR measurements in both the normal and SC states of FeSe_{1-x}S_x ($0 \leq x \leq 0.23$). A single crystal was used for each S-substitution level, and a magnetic field of 6.0 T was applied parallel to the FeSe plane to exclude the formation of vortices in the plane. T_c was determined from AC susceptibility measurements utilizing an NMR tank circuit. The susceptibility data are presented in detail in Supplementary Fig. 1 (see Supplementary Note 1); T_c for $x \leq 0.12$ was approximately 9 K, whereas T_c for $x = 0.18$ was 3 K at 6.0 T. ⁷⁷Se-NMR spectra for several S-substitution levels across $x_c \sim 0.17$ are shown later. Similarly to pure FeSe¹⁰, the NMR spectra showed double peaks or edges below the nematic transition temperature, T_{nem} , which merged into one peak with increasing S substitution.

Figure 1a shows the evolution of the relaxation rate divided by temperature ($1/T_1T$) with respect to S substitution, and Fig. 1b is a color plot of Fig. 1a. $1/T_1T$ provides a measure of low-energy spin fluctuations. In general, $1/T_1T$ is expressed as:

$$\frac{1}{T_1T} \sim \sum_{\mathbf{q}} \text{Im}\chi(\mathbf{q}) \quad (1)$$

where $\chi(\mathbf{q})$ is the wave-number (\mathbf{q})-dependent susceptibility. The T dependence of $1/T_1T$ shown in Fig. 1a contrasts with that of the Knight shift which is discussed later. The Knight shift, which reflects the uniform susceptibility $\chi(0)$, monotonically decreases with decreasing temperature. The upturns of $1/T_1T$ toward T_c originate from spin fluctuations with $\mathbf{q} \neq 0$. As shown in Fig. 1b, spin fluctuations develop remarkably in the nematic phase and

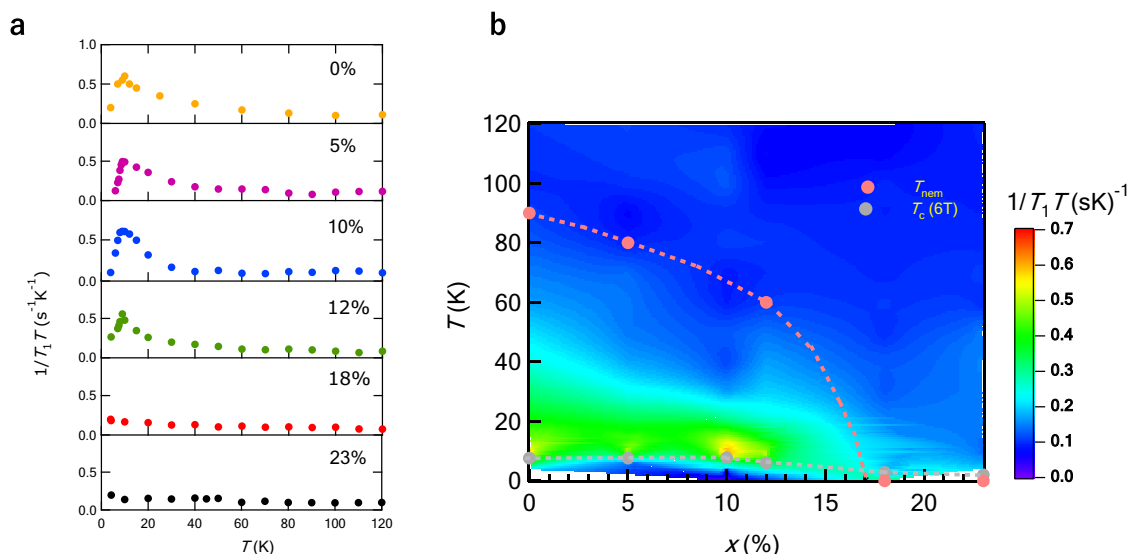


Fig. 1 ⁷⁷Se relaxation rate ($1/T_1$) divided by temperature (T) of FeSe_{1-x}S_x. **a** T dependence of $1/T_1T$ at high temperatures. The magnetic field of 6.0 T was applied parallel to the FeSe plane. The data for 12%-S-substituted FeSe were already published^{20,23}. **b** Color plot of $1/T_1T$. T_{nem} represents the nematic transition temperature, and $T_c(6\text{T})$ represents the superconducting (SC) transition temperature measured by means of the AC susceptibility at 6.0 T.

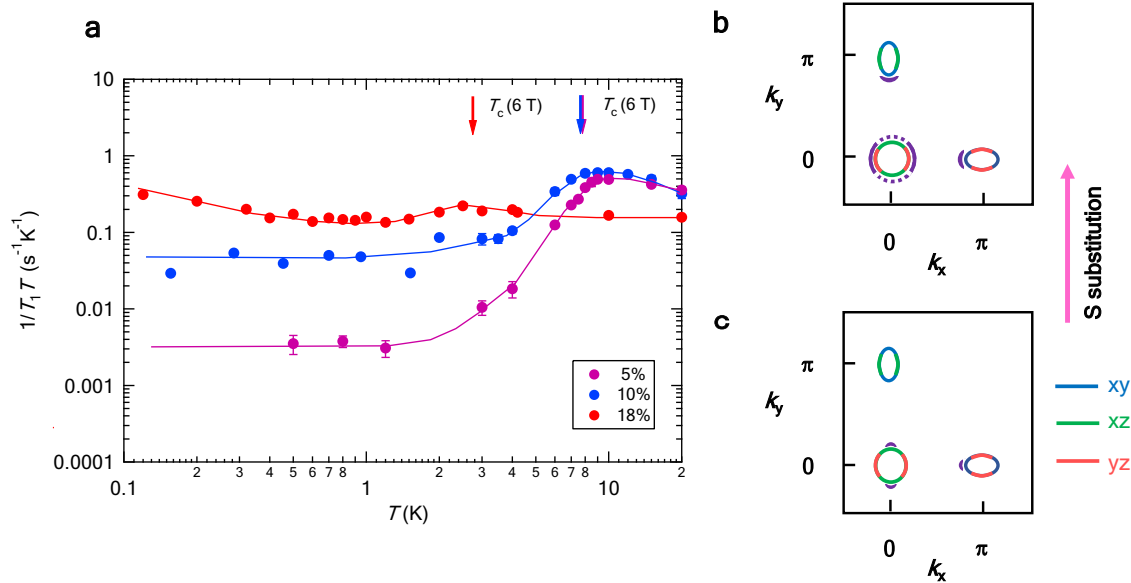


Fig. 2 $1/T_1T$ in the SC state and Bogoliubov Fermi surfaces (BFSs). **a** Temperature dependence of $1/T_1T$ at low temperatures below T_c for several S-substitution levels. Arrows indicate T_c measured at 6.0 T. Error bars are estimated from those of T_1 . All data points contain the error bars, although many of the error bars are smaller than the data points. **b** Schematic diagram of two-dimensional Fermi surfaces obtained theoretically for the tetragonal phase together with contributions from three orbitals, d_{xy} , d_{yz} and d_{zx} colored in blue, red, and green, respectively²⁵. Sufficiently expanded BFSs expected below T_c are colored in purple⁷. Recently, quasiparticle excitations with a finite gap has been observed for the directions shown by the dotted curves²⁹. **c** BFSs expanded from the nodal points of pure FeSe are colored in purple⁷.

are strongly suppressed in the tetragonal phase. Spin fluctuations are associated with the topological configuration of electron and hole pockets and interband couplings. Two-dimensional Fermi surfaces theoretically obtained in the tetragonal phase²⁵ are schematically shown in Fig. 2b, c. The enhancement of $\chi(\mathbf{q})$ is expected at $\mathbf{q} \sim (\pi, 0)$ in the nematic phase, as well as in the tetragonal phase, owing to the interband coupling between electron and hole pockets, namely, $\mathbf{q} = (\pi, 0)$ nesting. However, the absence of a magnetic order implies that the nesting is not very strong. Such weak coupling is expected when orbital-selective coupling becomes important. The experimental results in Fig. 1a are almost consistent with those observed by another study^{19,22}, wherein spin-fluctuation mediated pairing, that is, s^\pm -wave pairing was suggested because T_c reached a maximum for significantly strong spin fluctuations ($x \sim 0.1$)¹⁹.

Figure 2a shows $1/T_1T$ at temperatures below T_c for several S-substitution levels crossing $x_c \sim 0.17$, which is the main results in this study. The decrease in $1/T_1T$ below T_c is due to the opening of the SC gap. In conventional clean superconductors, $1/T_1T$ should decrease to zero with decreasing temperature. However, $1/T_1T$ for $x = 0.05$ and 0.10 became constant at low temperatures. With further substitution over x_c , $1/T_1T$ exhibited an upturn with decreasing temperature and the values became significantly larger than those for $x = 0.05$ and 0.10 . Upturns of $1/T_1T$ observed below and above T_c are very rare in SC systems. The low T behavior of $1/T_1T = \text{constant}$ suggests a residual DOS. As a cause of the residual DOS, (1) the impurity effect, (2) the Volovik effect, and (3) the coexistence of SC and normal states may be possible. First, the behavior of $1/T_1T = \text{constant}$ indicates an impurity effect in most cases. The impurity effect on $1/T_1$ has been studied theoretically at an early stage in the s^\pm -wave scenario²⁶.

For small impurity doping, the quasiparticle DOS is V-shaped as a function of energy, and the T dependence of $1/T_1T$ shows a T^2 dependence at temperatures below T_c . For fairly large impurity doping, the quasiparticle DOS has a finite value at zero energy, and $1/T_1T$ exhibits a T -independent relation followed by a T^2

dependence with decreasing temperature. At first, the impurity effect appears to explain the low T behavior of $1/T_1T$; however, this effect is excluded for the following reasons: (i) The upturn of $1/T_1T$ for $x = 0.18$ is difficult to explain, and (ii) impurity doping levels should be remarkably different between $x = 0.05$ and 0.10 because the constant value of $1/T_1T$ differs by approximately one order of magnitude. Therefore, T_c should be remarkably different between them. However, the value of T_c is almost the same between them. (iii) Furthermore, quantum oscillation measurements observed in a wide range of x covering the tetragonal phase indicates the relatively clean nature of the samples²⁷. The Volovik effect can also induce an in-gap state similarly to the impurity effect. The DOS can be induced by an applied field owing to the Doppler shift of quasiparticle energy. The field dependence of $1/T_1T$ has been theoretically investigated for s^\pm - and d -wave cases²⁸. This effect should result in almost the same $1/T_1T$ values between $x = 0.05$ and 0.10 , because the strength of the applied field is the same and the SC gap or T_c is almost the same between them. Therefore, this effect is excluded as well as the impurity effect. Another possibility is the coexistence of SC and normal states. The coexistence in real space implies that SC and normal metallic domains coexist. However, such a case can be excluded by the rather homogeneous spectra observed in the STS measurements⁵. Instead of the coexistence in real space, the coexistence in momentum space such as the formation of BFSs would be promising. BFSs that are expanded from the nodal points of pure FeSe and sufficiently expanded BFSs⁷ would play important roles for $x < x_c$ and $x > x_c$, respectively, in view of the STS and specific-heat results^{4,5}. The schematics of the former and latter are shown in Fig. 2c, b, respectively. In fact, BFSs should be much complicated because BFSs with two-fold symmetry have been suggested from recent ARPES measurements, although the measurements were performed for the tetragonal phase²⁹.

For small x , BFSs expanded from the nodal points are small, and the nesting is hardly expected, as shown in Fig. 2c. Therefore, the enhancement of $\chi(\mathbf{q})$ or the upturn of $1/T_1T$ is hardly expected, despite that such enhancement or upturn is caused in

the normal state due to the nesting between original Fermi surfaces. In such a case, flip flop of a nuclear spin due to scattering by quasiparticles becomes a major relaxation process, like the Korringa relation in conventional metals. The Korringa relation, $1/T_1TK_{\text{spin}}^2 = \text{constant}$, where K_{spin} is the spin part of the Knight shift K , is applied for conventional metals with free electrons or weakly interacting electrons. K is decomposed into K_{spin} and the orbital part K_{orb} ,

$$K = K_{\text{spin}} + K_{\text{orb}}, \quad (2)$$

where K_{spin} is proportional to the DOS and the uniform susceptibility $\chi(0)$. K_{spin} and K_{orb} can be separated at high temperatures using the susceptibility data, $\chi(0)$. K_{orb} is T -independent and is approximately 0.26% for $x = 0.12$ ²³. For conventional superconductors, K_{spin} approaches zero as temperature is decreased owing to the SC gap. In case considered in this study, K_{spin} remains nonzero due to the DOS of BFSs. Therefore, $1/T_1T$ can be expressed using the Korringa relation as follows despite of the SC state:

$$\frac{1}{T_1TK_{\text{spin}}^2} = \frac{4\pi k_B}{\hbar} \left(\frac{\gamma_n}{\gamma_e}\right)^2 K(\alpha) \quad (3)$$

where k_B and \hbar are the Boltzman and Planck constants, respectively, $\gamma_{n(e)}$ is the gyromagnetic ratio of ⁷⁷Se (electron), and $K(\alpha)$ is a function of the Stoner enhancement factor α . The Stoner factor is expressed as $\alpha = I\chi(0)$ where I represents the interaction coupling. $K(\alpha)$ provides a measure of electron correlation. For ferromagnetic metals, $K(\alpha) < 1$, whereas for antiferromagnetic metals, $K(\alpha) > 1$. Further, for free electrons, $\alpha = 0$ and $K(\alpha) = 1$. A detailed expression of $K(\alpha)$ is provided in Supplementary Note 2. As $1/T_1T$ for $x = 0.10$ is one order larger than that for $x = 0.05$,

K_{spin} estimated using Eq. (2) is approximately three times larger than that for $x = 0.05$. We estimated residual K_{spin} from the experimental results of $1/T_1T$, assuming that the interaction between quasiparticles is negligibly small, that is, $K(\alpha) = 1$. The value of K_{spin} is estimated to be 0.015% for $x = 0.05$. Subsequently, the ratio of K_{spin} between the SC and normal states is estimated to be 0.49, implying that the DOS of BFSs reaches almost half of the DOS observed in the normal state above T_c . In fact, certain quasiparticle correlations should exist ($K(\alpha) > 1$), and the value mentioned above is overestimated. To obtain a more precise estimation, a further theoretical analysis of $\chi(\mathbf{q})$ is required.

The estimation for $x = 0.05$ and 0.10 is not applicable for $x = 0.18$, because the Korringa relationship breaks. The nesting between sufficiently expanded BFSs can cause the enhancement of $\chi(\mathbf{q})$. A drop just below T_c originates from the opening of the SC gap and a rise just above T_c originates from spin fluctuations, which are strongly suppressed in the tetragonal phase. Interestingly, the T dependence of $1/T_1T$ below T_c is similar to that above T_c , although the magnitude of the upturn becomes one third across T_c . The T dependence of $\chi(\mathbf{q})$ at high temperatures originates from the nesting between original Fermi surfaces in the normal state. The reason why similar $\chi(\mathbf{q})$ is reestablished below T_c is that sufficiently expanded BFSs reflect original Fermi surfaces and a similar nesting becomes possible.

We have estimated K_{spin} from $1/T_1T$, however, it seems straightforward to estimate from K . Figure 3a shows the evolution of K with respect to S substitution. The results are almost consistent with those observed by another study¹⁹. In the nematic phase, two peaks appear reflecting two domains (the spectra of $x = 0.05$ and 0.12 in Fig. 3c). In Fig. 3a, only the average of the two peaks is plotted for temperatures below T_{nem} . The detailed

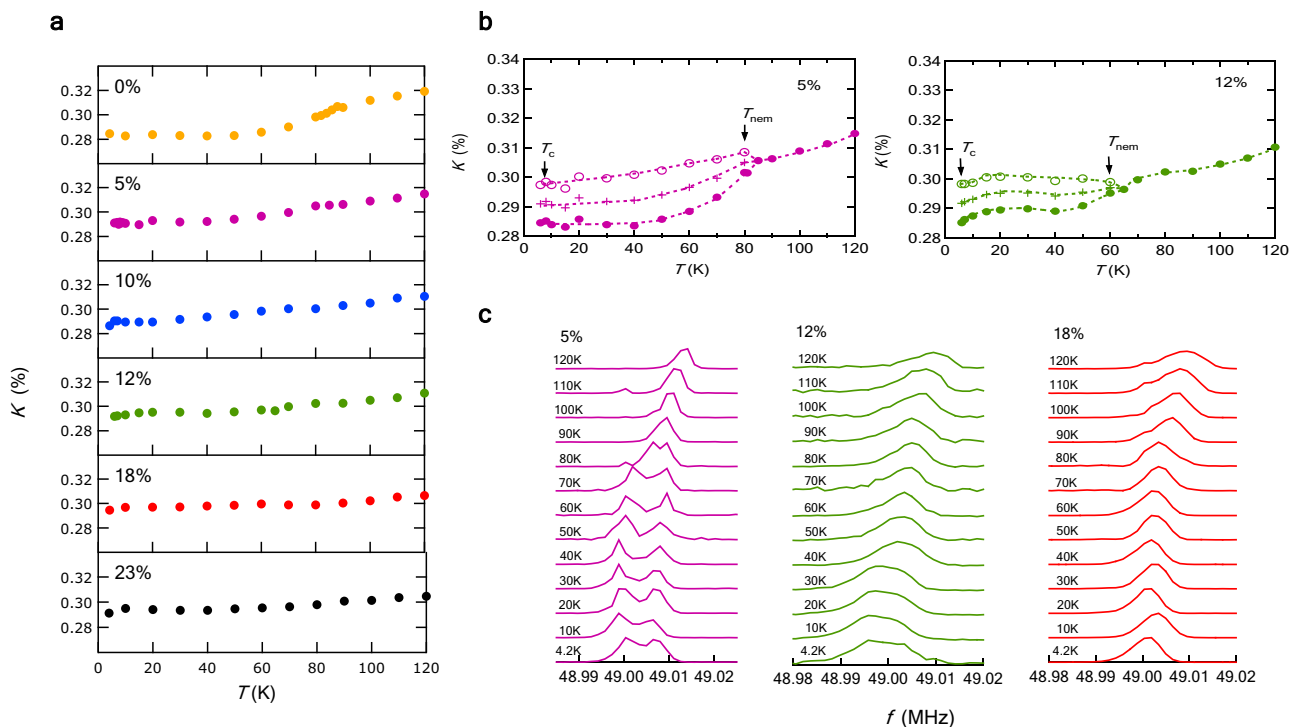


Fig. 3 ⁷⁷Se Knight shift (K) of $\text{FeSe}_{1-x}\text{S}_x$ determined from nuclear magnetic resonance (NMR) spectra. **a** Temperature dependence of K at high temperatures. The shifts were measured at the field (6.0 T) parallel to the FeSe plane. In the nematic phase ($x < 0.17$), two peaks or edges appear as shown in Fig. 3c. We plotted the average of two peaks for K below T_{nem} . The data for 12%-S-substituted sample ($x = 0.12$) was cited from the previous works^{20,23}. **b** K below T_{nem} for $x = 0.05$ and 0.12. T_{nem} and T_c represent the nematic and superconducting transition temperatures, respectively. Two peaks in Fig. 3c and their average are shown in both panels. Both panels are expansions of Fig. 3a. **c** ⁷⁷Se-NMR spectra for $x = 0.05$, 0.12, and 0.18. Two peaks appearing for $x = 0.05$ and 0.12 merge into a single peak with increasing S-substitution level over x_c (≥ 0.17).

shifts of each peak and their average are shown in Fig. 3b. Figure 3a certainly includes the information of $\chi(0)$ or K_{spin} . These quantities can be obtained from $K - \chi$ plots at high temperatures. This procedure is possible because both quantities are T -dependent at high temperatures (Fig. 3a). However, at very low temperatures below T_c , K_{spin} originating from the residual DOS and K_{orb} can not be separated from each other because both quantities are T -independent. Thus, a theoretical investigation is needed to separate K_{spin} from K_{orb} . Even if K_{orb} is theoretically calculated, small residual $K_{\text{spin}} (< 0.03)$ is estimated from the raw data, $K (\sim 0.28)$ by subtracting large $K_{\text{orb}} (\sim 0.25)$. This procedure can potentially contain a significant error. Furthermore, K_{orb} may change below and above T_{nem} in the lightly S-substituted regime, which renders the estimation of residual K_{spin} much more challenging. The estimation of K_{spin} from $1/T_1T$ is advantageous because the information on K_{orb} is not needed.

The low- T spin fluctuations above x_c can be attributed to the interband couplings between BFSs. However, the question arises as to whether the disappearance of the nematic order or revival of four-fold symmetry on the FeSe planes is essential for the couplings between BFSs. To investigate this problem, 12%-S-substituted FeSe at approximately 1 GPa may provide a clue because the T dependence of $1/T_1T$ is similar to that of 18%-S-substituted FeSe, that is, the suppression of spin fluctuations has been observed for 12%-S substitution at approximately 1 GPa^{20,23}. Further investigations at very low temperatures and high pressures are required for S-substituted FeSe ($x < x_c$).

Conclusion

In conclusion, we have observed anomalous spin fluctuations deep in the SC state for S-substituted FeSe over $x > x_c$ via $1/T_1T$ measurements to 100 mK, which suggests the presence of Bogoliubov quasiparticles. The upturn of $1/T_1T$ below T_c is similar to that above T_c , suggesting that $\chi(\mathbf{q})$ does not significantly change across T_c . Therefore, the upturn can be attributed to the enhancement of $\chi(\mathbf{q})$ due to the nesting between BFSs. This means that the expansion of BFSs is significantly large. The low- T spin fluctuations above x_c contrast with those below x_c arising from weakly interacting quasiparticles. The present NMR results highlight the novel SC state with BFSs, having excitations at zero energy.

Methods

We performed ^{77}Se -NMR measurements at 6.0 T using a single crystal for each S-substitution level. Typical size is approximately $1.0 \times 1.0 \times 0.5$ mm. We applied a magnetic field parallel to the FeSe planes to suppress the decrease in T_c and generation of vortices. We performed pulsed-NMR measurements using a conventional spectrometer. NMR spectra were obtained by the Fast Fourier Transform (FFT) of a spin-echo signal. To detect a echo signal, we used 4-cycle pulse sequence. The relaxation time (T_1) was measured by the saturation-recovery method, and the data points of the recovery curve were fitted by a single exponential function.

Data availability

The data that support the findings of this study are available from the corresponding author upon reasonable request.

Received: 16 January 2023; Accepted: 22 June 2023;

Published online: 13 July 2023

References

- Shibauchi, T., Hanaguri, T. & Matsuda, Y. Exotic superconducting states in FeSe-based materials. *J. Phys. Soc. Jpn.* **89**, 102002 (2020).
- Matsuura, K. et al. Maximizing T_c by tuning nematicity and magnetism in FeSe $_{1-x}$ S $_x$ superconductors. *Nat. Commun.* **8**, 1143 (2017).
- Hashimoto, T. et al. Superconducting gap anisotropy sensitive to nematic domains in FeSe. *Nat. Commun.* **9**, 282 (2018).

- Sato, Y. et al. Abrupt change of the superconducting gap structure at the nematic critical point in FeSe $_{1-x}$ S $_x$. *PNAS* **115**, 1227 (2018).
- Hanaguri, T. et al. Two distinct superconducting pairing states divided by the nematic end point in FeSe $_{1-x}$ S $_x$. *Sci. Adv.* **4**, eaar6419 (2018).
- Hanaguri, T. et al. Quantum vortex core and missing pseudogap in the multiband BCS-BEC crossover superconductor FeSe. *Phys. Rev. Lett.* **122**, 077001 (2019).
- Setty, C., Bhattacharyya, S., Cao, Y., Kreisel, A. & Hirshfeld, P. J. Topological ultranodal pair states in iron-based superconductors. *Nat. Commun.* **11**, 523 (2020).
- Setty, C., Cao, Y., Kreisel, A., Bhattacharyya, S. & Hirshfeld, P. J. Bogoliubov Fermi surfaces in spin-1/2 systems: Model Hamiltonians and experimental consequences. *Phys. Rev. B* **102**, 064504 (2020).
- Matsuura, K. et al. Two superconducting states with broken time-reversal symmetry in FeSe $_{1-x}$ S $_x$. *PNAS* **120**, e2208276120 (2023).
- Baek, S. H. et al. Orbital-driven nematicity in FeSe. *Nat. Mater.* **14**, 210 (2015).
- Wang, P. S. et al. Pressure induced stripe-order antiferromagnetism and first-order phase transition in FeSe. *Phys. Rev. Lett.* **117**, 237001 (2016).
- Li, J. et al. Spin-orbital-intertwined nematic state in FeSe. *Phys. Rev. X* **10**, 011034 (2020).
- Wiecki, P. et al. NMR evidence for static local nematicity and its cooperative interplay with low-energy magnetic fluctuations in FeSe under pressure. *Phys. Rev. B* **96**, 180502 (2017).
- Shi, A. et al. Pseudogap behavior of the nuclear spin-lattice relaxation rate in FeSe probed by ^{77}Se -NMR. *J. Phys. Soc. Jpn.* **87**, 013704 (2018).
- Zhou, R. et al. Singular magnetic anisotropy in the nematic phase of FeSe. *npj Quantum Mater.* **5**, 93 (2020).
- Molatta, S. et al. Superconductivity of highly spin-polarized electrons in FeSe probed by ^{77}Se NMR. *Phys. Rev. B* **104**, 014504 (2021).
- Vinograd, I. et al. Inhomogeneous Knight shift in vortex cores of superconducting FeSe. *Phys. Rev. B* **104**, 014502 (2021).
- Li, J. et al. ^{77}Se -NMR evidence for spin-singlet superconductivity with exotic superconducting fluctuations in FeSe. *Phys. Rev. B* **105**, 054514 (2022).
- Wiecki, P. et al. Persistent correlation between superconductivity and antiferromagnetic fluctuations near a nematic quantum critical point in FeSe $_{1-x}$ S $_x$. *Phys. Rev. B* **98**, 020507(R) (2018).
- Kuwayama, T. et al. ^{77}Se -NMR study under pressure on 12%-S doped FeSe. *J. Phys. Soc. Jpn.* **88**, 033703 (2019).
- Rana, K. et al. Impact of nematicity on the relationship between antiferromagnetic fluctuations and superconductivity in FeSe $_{0.91}\text{S}_{0.09}$ under pressure. *Phys. Rev. B* **101**, 180503 (2020).
- Baek, S. H. et al. Separate tuning of nematicity and spin fluctuations to unravel the origin of superconductivity in FeSe. *npj Quant. Mater.* **8**, 1 (2020).
- Kuwayama, T. et al. Pressure-induced reconstitution of Fermi surfaces and spin fluctuations in S-substituted FeSe. *Sci. Rep.* **11**, 17265 (2021).
- Rana, K. et al. Interrelationships between nematicity, antiferromagnetic spin fluctuations, and superconductivity: Role of hotspots in FeSe $_{1-x}$ S $_x$ revealed by high pressure ^{77}Se NMR study. *Phys. Rev. B* **107**, 134507 (2023).
- Yamakawa, Y. & Kontani, H. Nematicity, magnetism, and superconductivity in FeSe under pressure: Unified explanation based on the self-consistent vertex correction theory. *Phys. Rev. B* **96**, 144509 (2017).
- Bang, Y., Choi, H. Y. & Won, H. Impurity effects on the \pm s-wave state of the iron-based superconductors. *Phys. Rev. B* **79**, 054529 (2009).
- Coldea, A. I. et al. Evolution of the low-temperature Fermi surface of superconducting FeSe $_{1-x}$ S $_x$ across a nematic phase transition. *npj Quant. Mater.* **4**, 2 (2019).
- Bang, Y. Volovik effect on NMR measurements of unconventional superconductors. *Phys. Rev. B* **85**, 104524 (2012).
- Suzuki, T. et al. Discovery of nematic Bogoliubov Fermi surface in an iron-chalcogenide superconductor. <https://doi.org/10.21203/rs.3.rs-2224728/v1> (2022).

Acknowledgements

The authors would like to thank S. Nagasaki and T. Takahashi for their experimental support. The present work was supported by Grants-in-Aid for Scientific Research (KAKENHI Grant No. JP18H01181), JST SPRING, Grant Number JPMJSP2110, a grant from the Mitsubishi Foundation, and a grant from The Kyoto University Foundation. This work was partly supported by Grants-in-Aid for Scientific Research (KAKENHI Grant Nos. JP22H00105, JP18H05227, JP19H00648, and JP18K13492) and by Innovative Areas "Quantum Liquid Crystals" (No. JP19H05824) from the Japan Society for the Promotion of Science.

Author contributions

N.F. designed the NMR experiments. Z.Y., K.N., and K.I. carried out the NMR measurements. K.M., Y. Mizukami, S.K., Y. Matsuda, and T.S. synthesized the samples and performed the chemical analysis of the samples. X.S. and T.M. operated the dilution refrigerator to cool down to 100 mK under the instruction of Y. Uwatoko.

Competing interests

The authors declare no competing interests.

Additional information

Supplementary information The online version contains supplementary material available at <https://doi.org/10.1038/s42005-023-01286-x>.

Correspondence and requests for materials should be addressed to Naoki Fujiwara.

Peer review information *Communications Physics* thanks Chandan Setty and the other, anonymous, reviewer(s) for their contribution to the peer review of this work.

Reprints and permission information is available at <http://www.nature.com/reprints>

Publisher's note Springer Nature remains neutral with regard to jurisdictional claims in published maps and institutional affiliations.



Open Access This article is licensed under a Creative Commons Attribution 4.0 International License, which permits use, sharing, adaptation, distribution and reproduction in any medium or format, as long as you give appropriate credit to the original author(s) and the source, provide a link to the Creative Commons license, and indicate if changes were made. The images or other third party material in this article are included in the article's Creative Commons license, unless indicated otherwise in a credit line to the material. If material is not included in the article's Creative Commons license and your intended use is not permitted by statutory regulation or exceeds the permitted use, you will need to obtain permission directly from the copyright holder. To view a copy of this license, visit <http://creativecommons.org/licenses/by/4.0/>.

© The Author(s) 2023